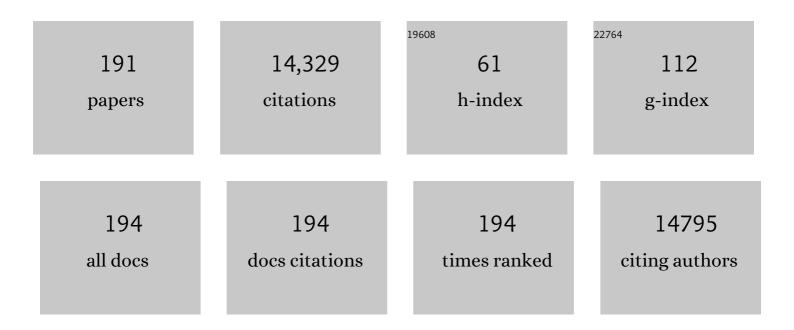


List of Publications by Year in descending order

Source: https://exaly.com/author-pdf/3232979/publications.pdf Version: 2024-02-01



Ιτιν Υιν

#	Article	IF	CITATIONS
1	Managing grains and interfaces via ligand anchoring enables 22.3%-efficiency inverted perovskite solar cells. Nature Energy, 2020, 5, 131-140.	19.8	894
2	Bidentate Ligand-Passivated CsPbI ₃ Perovskite Nanocrystals for Stable Near-Unity Photoluminescence Quantum Yield and Efficient Red Light-Emitting Diodes. Journal of the American Chemical Society, 2018, 140, 562-565.	6.6	745
3	State of the Art and Prospects for Halide Perovskite Nanocrystals. ACS Nano, 2021, 15, 10775-10981.	7.3	705
4	Lead iodide perovskite light-emitting field-effect transistor. Nature Communications, 2015, 6, 7383.	5.8	641
5	Lead-Free MA ₂ CuCl _{<i>x</i>} Br _{4–<i>x</i>} Hybrid Perovskites. Inorganic Chemistry, 2016, 55, 1044-1052.	1.9	457
6	Ultralow Self-Doping in Two-dimensional Hybrid Perovskite Single Crystals. Nano Letters, 2017, 17, 4759-4767.	4.5	251
7	Identifying the Molecular Structures of Intermediates for Optimizing the Fabrication of High-Quality Perovskite Films. Journal of the American Chemical Society, 2016, 138, 9919-9926.	6.6	249
8	Giant Photoluminescence Enhancement in CsPbCl ₃ Perovskite Nanocrystals by Simultaneous Dual-Surface Passivation. ACS Energy Letters, 2018, 3, 2301-2307.	8.8	244
9	Investigating the Origin of Enhanced C ₂₊ Selectivity in Oxide-/Hydroxide-Derived Copper Electrodes during CO ₂ Electroreduction. Journal of the American Chemical Society, 2020, 142, 4213-4222.	6.6	236
10	Well-Defined Thiolated Nanographene as Hole-Transporting Material for Efficient and Stable Perovskite Solar Cells. Journal of the American Chemical Society, 2015, 137, 10914-10917.	6.6	229
11	Chlorine Vacancy Passivation in Mixed Halide Perovskite Quantum Dots by Organic Pseudohalides Enables Efficient Rec. 2020 Blue Light-Emitting Diodes. ACS Energy Letters, 2020, 5, 793-798.	8.8	208
12	Unprecedented Ultralow Detection Limit of Amines using a Thiadiazole-Functionalized Zr(IV)-Based Metal–Organic Framework. Journal of the American Chemical Society, 2019, 141, 7245-7249.	6.6	203
13	Concentrated dual-cation electrolyte strategy for aqueous zinc-ion batteries. Energy and Environmental Science, 2021, 14, 4463-4473.	15.6	203
14	Inside Perovskites: Quantum Luminescence from Bulk Cs ₄ PbBr ₆ Single Crystals. Chemistry of Materials, 2017, 29, 7108-7113.	3.2	200
15	Polaron self-localization in white-light emitting hybrid perovskites. Journal of Materials Chemistry C, 2017, 5, 2771-2780.	2.7	196
16	Molecular behavior of zero-dimensional perovskites. Science Advances, 2017, 3, e1701793.	4.7	187
17	Novel hole transporting materials based on triptycene core for high efficiency mesoscopic perovskite solar cells. Chemical Science, 2014, 5, 2702-2709.	3.7	180
18	Thiols as interfacial modifiers to enhance the performance and stability of perovskite solar cells. Nanoscale, 2015, 7, 9443-9447.	2.8	179

#	Article	IF	CITATIONS
19	Tunable Multipolar Surface Plasmons in 2D Ti ₃ C ₂ <i>T</i> _{<i>x</i>} MXene Flakes. ACS Nano, 2018, 12, 8485-8493.	7.3	179
20	Room-Temperature Engineering of All-Inorganic Perovskite Nanocrsytals with Different Dimensionalities. Chemistry of Materials, 2017, 29, 8978-8982.	3.2	174
21	Direct-Indirect Nature of the Bandgap in Lead-Free Perovskite Nanocrystals. Journal of Physical Chemistry Letters, 2017, 8, 3173-3177.	2.1	172
22	White light emission in low-dimensional perovskites. Journal of Materials Chemistry C, 2019, 7, 4956-4969.	2.7	163
23	Contribution of Metal Defects in the Assembly Induced Emission of Cu Nanoclusters. Journal of the American Chemical Society, 2017, 139, 4318-4321.	6.6	152
24	Monoammonium Porphyrin for Blade-Coating Stable Large-Area Perovskite Solar Cells with >18% Efficiency. Journal of the American Chemical Society, 2019, 141, 6345-6351.	6.6	149
25	Point Defects and Green Emission in Zero-Dimensional Perovskites. Journal of Physical Chemistry Letters, 2018, 9, 5490-5495.	2.1	143
26	Interfacial Charge Transfer Anisotropy in Polycrystalline Lead Iodide Perovskite Films. Journal of Physical Chemistry Letters, 2015, 6, 1396-1402.	2.1	141
27	Excitonic and Polaronic Properties of 2D Hybrid Organic–Inorganic Perovskites. ACS Energy Letters, 2017, 2, 417-423.	8.8	140
28	Extremely reduced dielectric confinement in two-dimensional hybrid perovskites with large polar organics. Communications Physics, 2018, 1, .	2.0	135
29	Intrinsic Lead Ion Emissions in Zero-Dimensional Cs ₄ PbBr ₆ Nanocrystals. ACS Energy Letters, 2017, 2, 2805-2811.	8.8	133
30	Assembly of Atomically Precise Silver Nanoclusters into Nanocluster-Based Frameworks. Journal of the American Chemical Society, 2019, 141, 9585-9592.	6.6	132
31	CsPb ₂ Br ₅ Single Crystals: Synthesis and Characterization. ChemSusChem, 2017, 10, 3746-3749.	3.6	130
32	Enhancing Organic Phosphorescence by Manipulating Heavy-Atom Interaction. Crystal Growth and Design, 2016, 16, 808-813.	1.4	122
33	Halogen Migration in Hybrid Perovskites: The Organic Cation Matters. Journal of Physical Chemistry Letters, 2018, 9, 5474-5480.	2.1	119
34	Light-Induced Self-Assembly of Cubic CsPbBr ₃ Perovskite Nanocrystals into Nanowires. Chemistry of Materials, 2019, 31, 6642-6649.	3.2	119
35	The Benefit and Challenges of Zero-Dimensional Perovskites. Journal of Physical Chemistry Letters, 2018, 9, 4131-4138.	2.1	118
36	Highly Stable Phosphonateâ€Based MOFs with Engineered Bandgaps for Efficient Photocatalytic Hydrogen Production. Advanced Materials, 2020, 32, e1906368.	11.1	117

#	Article	IF	CITATIONS
37	Unlocking the Effect of Trivalent Metal Doping in All-Inorganic CsPbBr ₃ Perovskite. ACS Energy Letters, 2019, 4, 789-795.	8.8	116
38	Energy Transfer in Metal–Organic Frameworks for Fluorescence Sensing. ACS Applied Materials & Interfaces, 2022, 14, 9970-9986.	4.0	109
39	Phase-change-driven dielectric-plasmonic transitions in chalcogenide metasurfaces. NPG Asia Materials, 2018, 10, 533-539.	3.8	108
40	Sulfonate-Assisted Surface lodide Management for High-Performance Perovskite Solar Cells and Modules. Journal of the American Chemical Society, 2021, 143, 10624-10632.	6.6	101
41	Pyridine-Induced Dimensionality Change in Hybrid Perovskite Nanocrystals. Chemistry of Materials, 2017, 29, 4393-4400.	3.2	100
42	Successes and Challenges of Core/Shell Lead Halide Perovskite Nanocrystals. ACS Energy Letters, 2021, 6, 1340-1357.	8.8	100
43	28.2%-efficient, outdoor-stable perovskite/silicon tandem solar cell. Joule, 2021, 5, 3169-3186.	11.7	99
44	Tuning Hot Carrier Cooling Dynamics by Dielectric Confinement in Two-Dimensional Hybrid Perovskite Crystals. ACS Nano, 2019, 13, 12621-12629.	7.3	96
45	Improved stability of perovskite solar cells in ambient air by controlling the mesoporous layer. Journal of Materials Chemistry A, 2015, 3, 16860-16866.	5.2	92
46	Layer-Dependent Rashba Band Splitting in 2D Hybrid Perovskites. Chemistry of Materials, 2018, 30, 8538-8545.	3.2	92
47	Single Crystals: The Next Big Wave of Perovskite Optoelectronics. , 2020, 2, 184-214.		89
48	Chemically Stable Guanidinium Covalent Organic Framework for the Efficient Capture of Low-Concentration Iodine at High Temperatures. Journal of the American Chemical Society, 2022, 144, 6821-6829.	6.6	89
49	Defect Passivation in Perovskite Solar Cells by Cyanoâ€Based Ï€â€Conjugated Molecules for Improved Performance and Stability. Advanced Functional Materials, 2020, 30, 2002861.	7.8	87
50	CsMnBr ₃ : Lead-Free Nanocrystals with High Photoluminescence Quantum Yield and Picosecond Radiative Lifetime. , 2021, 3, 290-297.		86
51	Ultralong Radiative States in Hybrid Perovskite Crystals: Compositions for Submillimeter Diffusion Lengths. Journal of Physical Chemistry Letters, 2017, 8, 4386-4390.	2.1	83
52	Ag nanoparticle/ZnO hollow nanosphere arrays: large scale synthesis and surface plasmon resonance effect induced Raman scattering enhancement. Journal of Materials Chemistry, 2012, 22, 7902.	6.7	82
53	[Cu ₈₁ (PhS) ₄₆ (^{<i>t</i>} BuNH ₂) ₁₀ (H) _{32< Reveals the Coexistence of Large Planar Cores and Hemispherical Shells in High-Nuclearity Copper Nanoclusters. Journal of the American Chemical Society, 2020, 142, 8696-8705.}	:/sub>] <su 6.6</su 	up>3+ 81
54	Vapor-assisted crystallization control toward high performance perovskite photovoltaics with over 18% efficiency in the ambient atmosphere. Journal of Materials Chemistry A, 2016, 4, 13203-13210.	5.2	77

#	Article	IF	CITATIONS
55	Recent Advances on Conductive 2D Covalent Organic Frameworks. Small, 2021, 17, e2006043.	5.2	77
56	Self-Optimized Metal–Organic Framework Electrocatalysts with Structural Stability and High Current Tolerance for Water Oxidation. ACS Catalysis, 2021, 11, 7132-7143.	5.5	77
57	Linked Nickel Oxide/Perovskite Interface Passivation for Highâ€Performance Textured Monolithic Tandem Solar Cells. Advanced Energy Materials, 2021, 11, 2101662.	10.2	77
58	Characterization of the Valence and Conduction Band Levels of <i>n</i> = 1 2D Perovskites: A Combined Experimental and Theoretical Investigation. Advanced Energy Materials, 2018, 8, 1703468.	10.2	76
59	Conjugated Asymmetric Donor‣ubstituted 1,3,5â€īriazines: New Host Materials for Blue Phosphorescent Organic Lightâ€Emitting Diodes. Chemistry - A European Journal, 2011, 17, 10871-10878.	1.7	75
60	Modulation of Broadband Emissions in Two-Dimensional ⟠100⟩-Oriented Ruddlesden–Popper Hybrid Perovskites. ACS Energy Letters, 2020, 5, 2149-2155.	8.8	75
61	Perovskite-Nanosheet Sensitizer for Highly Efficient Organic X-ray Imaging Scintillator. ACS Energy Letters, 2022, 7, 10-16.	8.8	72
62	Tuning the Optoelectronic Properties of 4,4′- <i>N</i> , <i>N</i> ′-Dicarbazole-biphenyl through Heteroatom Linkage: New Host Materials for Phosphorescent Organic Light-Emitting Diodes. Organic Letters, 2010, 12, 3438-3441.	2.4	71
63	Lead-free, stable, high-efficiency (52%) blue luminescent FA ₃ Bi ₂ Br ₉ perovskite quantum dots. Nanoscale Horizons, 2020, 5, 580-585.	4.1	70
64	Plasmonics of topological insulators at optical frequencies. NPG Asia Materials, 2017, 9, e425-e425.	3.8	65
65	Ligand-Free Nanocrystals of Highly Emissive Cs ₄ PbBr ₆ Perovskite. Journal of Physical Chemistry C, 2018, 122, 6493-6498.	1.5	63
66	Layer-edge device of two-dimensional hybrid perovskites. Nature Communications, 2018, 9, 5196.	5.8	63
67	Exceptional Blueshifted and Enhanced Aggregationâ€Induced Emission of Conjugated Asymmetric Triazines and Their Applications in Superamplified Detection of Explosives. Chemistry - A European Journal, 2012, 18, 15655-15661.	1.7	60
68	Theoretical Studies of the Structural, Electronic, and Optical Properties of Phosphafluorenes. Journal of Physical Chemistry A, 2010, 114, 3655-3667.	1.1	59
69	Methylamine-Dimer-Induced Phase Transition toward MAPbI ₃ Films and High-Efficiency Perovskite Solar Modules. Journal of the American Chemical Society, 2020, 142, 6149-6157.	6.6	59
70	Perovskite Quantum Dots as Multifunctional Interlayers in Perovskite Solar Cells with Dopant-Free Organic Hole Transporting Layers. Journal of the American Chemical Society, 2021, 143, 5855-5866.	6.6	59
71	Lecithin Capping Ligands Enable Ultrastable Perovskite-Phase CsPbI ₃ Quantum Dots for Rec. 2020 Bright-Red Light-Emitting Diodes. Journal of the American Chemical Society, 2022, 144, 13302-13310.	6.6	59
72	Tellurium-Based Double Perovskites A ₂ TeX ₆ with Tunable Band Gap and Long Carrier Diffusion Length for Optoelectronic Applications. ACS Energy Letters, 2019, 4, 228-234.	8.8	58

#	Article	IF	CITATIONS
73	Compositionally Screened Eutectic Catalytic Coatings on Halide Perovskite Photocathodes for Photoassisted Selective CO ₂ Reduction. ACS Energy Letters, 2019, 4, 1279-1286.	8.8	56
74	Manipulating crystallization dynamics through chelating molecules for bright perovskite emitters. Nature Communications, 2021, 12, 4831.	5.8	56
75	Visible Range Plasmonic Modes on Topological Insulator Nanostructures. Advanced Optical Materials, 2017, 5, 1600768.	3.6	55
76	Why are Hot Holes Easier to Extract than Hot Electrons from Methylammonium Lead Iodide Perovskite?. Advanced Energy Materials, 2019, 9, 1900084.	10.2	54
77	Nearly 100% energy transfer at the interface of metal-organic frameworks for X-ray imaging scintillators. Matter, 2022, 5, 253-265.	5.0	53
78	Carbazole endcapped heterofluorenes as host materials: theoretical study of their structural, electronic, and optical properties. Physical Chemistry Chemical Physics, 2010, 12, 15448.	1.3	51
79	Defect-Triggered Phase Transition in Cesium Lead Halide Perovskite Nanocrystals. , 2019, 1, 185-191.		51
80	Crown Etherâ€Assisted Growth and Scaling Up of FACsPbl ₃ Films for Efficient and Stable Perovskite Solar Modules. Advanced Functional Materials, 2021, 31, 2008760.	7.8	50
81	[Cu ₁₅ (PPh ₃) ₆ (PET) ₁₃] ²⁺ : a Copper Nanocluster with Crystallization Enhanced Photoluminescence. Small, 2021, 17, e2006839.	5.2	50
82	Effect of Zincâ€Doping on the Reduction of the Hotâ€Carrier Cooling Rate in Halide Perovskites. Angewandte Chemie - International Edition, 2021, 60, 10957-10963.	7.2	50
83	Exciton Self-Trapping for White Emission in 100-Oriented Two-Dimensional Perovskites via Halogen Substitution. ACS Energy Letters, 2022, 7, 453-460.	8.8	50
84	Light-induced activation of boron doping in hydrogenated amorphous silicon for over 25% efficiency silicon solar cells. Nature Energy, 2022, 7, 427-437.	19.8	50
85	Facile Synthesis of a Furan–Arylamine Holeâ€Transporting Material for Highâ€Efficiency, Mesoscopic Perovskite Solar Cells. Chemistry - A European Journal, 2015, 21, 15113-15117.	1.7	49
86	Halogen Vacancies Enable Ligandâ€Assisted Selfâ€Assembly of Perovskite Quantum Dots into Nanowires. Angewandte Chemie - International Edition, 2019, 58, 16077-16081.	7.2	49
87	Theory-Guided Synthesis of Highly Luminescent Colloidal Cesium Tin Halide Perovskite Nanocrystals. Journal of the American Chemical Society, 2021, 143, 5470-5480.	6.6	49
88	Installation of synergistic binding sites onto porous organic polymers for efficient removal of perfluorooctanoic acid. Nature Communications, 2022, 13, 2132.	5.8	49
89	Inner salt-shaped small molecular photosensitizer with extremely enhanced two-photon absorption for mitochondrial-targeted photodynamic therapy. Chemical Communications, 2017, 53, 1680-1683.	2.2	46
90	Boosting Self-Trapped Emissions in Zero-Dimensional Perovskite Heterostructures. Chemistry of Materials, 2020, 32, 5036-5043.	3.2	46

#	Article	IF	CITATIONS
91	Plasmonic-enhanced self-cleaning activity on asymmetric Ag/ZnO surface-enhanced Raman scattering substrates under UV and visible light irradiation. Journal of Materials Chemistry A, 2014, 2, 7747-7753.	5.2	45
92	Infrared dielectric metamaterials from high refractive index chalcogenides. Nature Communications, 2020, 11, 1692.	5.8	45
93	Effect of the surface-plasmon–exciton coupling and charge transfer process on the photoluminescence of metal–semiconductor nanostructures. Nanoscale, 2013, 5, 4436.	2.8	43
94	Near-unity photoluminescence quantum yield in inorganic perovskite nanocrystals by metal-ion doping. Journal of Chemical Physics, 2020, 152, 020902.	1.2	42
95	Doping Induces Structural Phase Transitions in All-Inorganic Lead Halide Perovskite Nanocrystals. , 2020, 2, 367-375.		42
96	Emergence of multiple fluorophores in individual cesium lead bromide nanocrystals. Nature Communications, 2019, 10, 2930.	5.8	41
97	[Cu ₂₃ (PhSe) ₁₆ (Ph ₃ P) ₈ (H) ₆] · BF _{ Atomic-Level Insights into Cuboidal Polyhydrido Copper Nanoclusters and Their Quasi-simple Cubic Self-Assembly. , 2021, 3, 90-99.}	4:	41
98	Manipulation of hot carrier cooling dynamics in two-dimensional Dion–Jacobson hybrid perovskites via Rashba band splitting. Nature Communications, 2021, 12, 3995.	5.8	41
99	MAPbl ₃ Single Crystals Free from Hole-Trapping Centers for Enhanced Photodetectivity. ACS Energy Letters, 2019, 4, 2579-2584.	8.8	40
100	Ag ₂ S Quantum Dots as an Infrared Excited Photocatalyst for Hydrogen Production. ACS Applied Energy Materials, 2019, 2, 2751-2759.	2.5	40
101	Br-containing alkyl ammonium salt-enabled scalable fabrication of high-quality perovskite films for efficient and stable perovskite modules. Journal of Materials Chemistry A, 2019, 7, 26849-26857.	5.2	40
102	Multiple exciton generation in tin–lead halide perovskite nanocrystals for photocurrent quantum efficiency enhancement. Nature Photonics, 2022, 16, 485-490.	15.6	40
103	Engineered tunneling layer with enhanced impact ionization for detection improvement in graphene/silicon heterojunction photodetectors. Light: Science and Applications, 2021, 10, 113.	7.7	39
104	Layer-Dependent Coherent Acoustic Phonons in Two-Dimensional Ruddlesden–Popper Perovskite Crystals. Journal of Physical Chemistry Letters, 2019, 10, 5259-5264.	2.1	38
105	Facile synthesis of a hole transporting material with a silafluorene core for efficient mesoscopic CH ₃ NH ₃ PbI ₃ perovskite solar cells. Journal of Materials Chemistry A, 2016, 4, 8750-8754.	5.2	36
106	Large Polaron Self-Trapped States in Three-Dimensional Metal-Halide Perovskites. , 2020, 2, 20-27.		33
107	Surface Plasmon Enhanced Hot Exciton Emission in Deep UVâ€Emitting AlGaN Multiple Quantum Wells. Advanced Optical Materials, 2014, 2, 451-458.	3.6	32
108	Luminescence and Stability Enhancement of Inorganic Perovskite Nanocrystals via Selective Surface Ligand Binding. ACS Nano, 2021, 15, 17998-18005.	7.3	32

#	Article	IF	CITATIONS
109	Self-assembled hollow nanosphere arrays used as low Q whispering gallery mode resonators on thin film solar cells for light trapping. Physical Chemistry Chemical Physics, 2013, 15, 16874.	1.3	31
110	Hydrated Mg <i>_x</i> V ₅ O ₁₂ Cathode with Improved Mg ²⁺ Storage Performance. Advanced Energy Materials, 2020, 10, 2002128.	10.2	31
111	An Aqueous Mg ²⁺ â€Based Dualâ€Ion Battery with High Power Density. Advanced Functional Materials, 2021, 31, 2107523.	7.8	30
112	Novel heterofluorene-based hosts for highly efficient blue electrophosphorescence at low operating voltages. Organic Electronics, 2011, 12, 1619-1624.	1.4	29
113	Unprecedented Surface Plasmon Modes in Monoclinic MoO ₂ Nanostructures. Advanced Materials, 2020, 32, e1908392.	11.1	28
114	Multipole plasmon resonances in self-assembled metal hollow-nanospheres. Nanoscale, 2014, 6, 3934-3940.	2.8	27
115	Femtosecond to Microsecond Dynamics of Soret-Band Excited Corroles. Journal of Physical Chemistry C, 2015, 119, 28691-28700.	1.5	27
116	High-mobility patternable MoS2 percolating nanofilms. Nano Research, 2021, 14, 2255.	5.8	27
117	Structure-controlled optical thermoresponse in Ruddlesden-Popper layered perovskites. APL Materials, 2018, 6, .	2.2	26
118	First-Principles Study of the Nuclear Dynamics of Doped Conjugated Polymers. Journal of Physical Chemistry C, 2016, 120, 1994-2001.	1.5	25
119	Light absorption enhancement by embedding submicron scattering TiO ₂ nanoparticles in perovskite solar cells. RSC Advances, 2016, 6, 24596-24602.	1.7	25
120	Theoretical Study of Charge-Transfer Properties of the π-Stacked Poly(1,1-silafluorene)s. Journal of Physical Chemistry C, 2011, 115, 14778-14785.	1.5	24
121	Trace surface-clean palladium nanosheets as a conductivity enhancer in hole-transporting layers to improve the overall performances of perovskite solar cells. Nanoscale, 2016, 8, 3274-3277.	2.8	24
122	Engineering Surface Orientations for Efficient and Stable Hybrid Perovskite Single-Crystal Solar Cells. ACS Energy Letters, 2022, 7, 1544-1552.	8.8	24
123	Shining Light on the Structure of Lead Halide Perovskite Nanocrystals. , 2021, 3, 845-861.		23
124	Metal–Organic Frameworks in Mixed-Matrix Membranes for High-Speed Visible-Light Communication. Journal of the American Chemical Society, 2022, 144, 6813-6820.	6.6	23
125	Theoretical study of organic molecules containing N or S atoms as receptors for Hg(II) fluorescent sensors. Synthetic Metals, 2012, 162, 641-649.	2.1	22
126	Charge Redistribution at GaAs/P3HT Heterointerfaces with Different Surface Polarity. Journal of Physical Chemistry Letters, 2013, 4, 3303-3309.	2.1	22

#	Article	IF	CITATIONS
127	Synergetic SERS Enhancement in a Metal-Like/Metal Double-Shell Structure for Sensitive and Stable Application. ACS Applied Materials & Interfaces, 2017, 9, 13564-13570.	4.0	22
128	Luminescent Copper(I) Halides for Optoelectronic Applications. Physica Status Solidi - Rapid Research Letters, 2021, 15, 2100138.	1.2	22
129	Extraordinary Carrier Diffusion on CdTe Surfaces Uncovered by 4D Electron Microscopy. CheM, 2019, 5, 706-718.	5.8	21
130	Air-Resistant Lead Halide Perovskite Nanocrystals Embedded into Polyimide of Intrinsic Microporosity. Energy Material Advances, 2021, 2021, .	4.7	21
131	Zincophilic Laserâ€5cribed Graphene Interlayer for Homogeneous Zinc Deposition and Stable Zincâ€lon Batteries. Energy Technology, 2021, 9, 2100490.	1.8	21
132	Resonanceâ€Mediated Dynamic Modulation of Perovskite Crystallization for Efficient and Stable Solar Cells. Advanced Materials, 2022, 34, e2107111.	11.1	21
133	Mapping polarons in polymer FETs by charge modulation microscopy in the mid-infrared. Scientific Reports, 2014, 4, 3626.	1.6	18
134	Highly efficient and stable blueâ€lightâ€emitting binaphtholâ€fluorene copolymers: A joint experimental and theoretical study of the mainâ€chain chirality. Journal of Polymer Science Part A, 2010, 48, 3868-3879.	2.5	17
135	Growth-Dynamic-Controllable Rapid Crystallization Boosts the Perovskite Photovoltaics' Robust Preparation: From Blade Coating to Painting. ACS Applied Materials & Interfaces, 2018, 10, 23103-23111.	4.0	17
136	Synergistic Effect between NiO <i>_x</i> and P3HT Enabling Efficient and Stable Hole Transport Pathways for Regular Perovskite Photovoltaics. Advanced Functional Materials, 2022, 32, .	7.8	17
137	Engineering a Kesteriteâ€Based Photocathode for Photoelectrochemical Ammonia Synthesis from NO <i>_x</i> Reduction. Advanced Materials, 2022, 34, .	11.1	17
138	Halogen Vacancies Enable Ligandâ€Assisted Selfâ€Assembly of Perovskite Quantum Dots into Nanowires. Angewandte Chemie, 2019, 131, 16223-16227.	1.6	16
139	Cyanamide Passivation Enables Robust Elemental Imaging of Metal Halide Perovskites at Atomic Resolution. Journal of Physical Chemistry Letters, 2021, 12, 10402-10409.	2.1	15
140	3D CoMoSe4 Nanosheet Arrays Converted Directly from Hydrothermally Processed CoMoO4 Nanosheet Arrays by Plasma-Assisted Selenization Process Toward Excellent Anode Material in Sodium-Ion Battery. Nanoscale Research Letters, 2019, 14, 213.	3.1	14
141	Tunable Twisting Motion of Organic Linkers via Concentration and Hydrogen-Bond Formation. Journal of Physical Chemistry C, 2019, 123, 5900-5906.	1.5	14
142	Reduced ion migration and enhanced photoresponse in cuboid crystals of methylammonium lead iodide perovskite. Journal Physics D: Applied Physics, 2019, 52, 054001.	1.3	14
143	Interface Matters: Enhanced Photoluminescence and Long-Term Stability of Zero-Dimensional Cesium Lead Bromide Nanocrystals <i>via</i> Gas-Phase Aluminum Oxide Encapsulation. ACS Applied Materials & Interfaces, 2020, 12, 35598-35605.	4.0	14
144	Manipulation of the crystallization of perovskite films induced by a rotating magnetic field during blade coating in air. Journal of Materials Chemistry A, 2018, 6, 3986-3995.	5.2	13

#	Article	IF	CITATIONS
145	Highâ€Resolution Printable and Elastomeric Conductors from Strainâ€Adaptive Assemblies of Metallic Nanoparticles with Low Aspect Ratios. Small, 2020, 16, 2004793.	5.2	13
146	Hyperstable Perovskite Solar Cells Without Ion Migration and Metal Diffusion Based on ZnS Segregated Cubic ZnTiO ₃ Electron Transport Layers. Solar Rrl, 2021, 5, 2000654.	3.1	13
147	Cascade Electron Transfer Induces Slow Hot Carrier Relaxation in CsPbBr ₃ Asymmetric Quantum Wells. ACS Energy Letters, 2021, 6, 2602-2609.	8.8	13
148	Scalable Preparation of Highâ€Performance ZnO–SnO ₂ Cascaded Electron Transport Layer for Efficient Perovskite Solar Modules. Solar Rrl, 2022, 6, 2100639.	3.1	13
149	Interface Engineering of Cubic Zinc Metatitanate as an Excellent Electron Transport Material for Stable Perovskite Solar Cells. Solar Rrl, 2020, 4, 1900533.	3.1	12
150	Real-Space Mapping of Surface-Oxygen Defect States in Photovoltaic Materials Using Low-Voltage Scanning Ultrafast Electron Microscopy. ACS Applied Materials & Interfaces, 2020, 12, 7760-7767.	4.0	12
151	Polarization-Controllable Plasmonic Enhancement on the Optical Response of Two-Dimensional GaSe Layers. ACS Applied Materials & Interfaces, 2019, 11, 19631-19637.	4.0	11
152	Small-Size Effects on Electron Transfer in P3HT/InP Quantum Dots. Journal of Physical Chemistry C, 2015, 119, 26783-26792.	1.5	10
153	Photoresponsive azobenzene ligand as an efficient electron acceptor for luminous CdTe quantum dots. Journal of Photochemistry and Photobiology A: Chemistry, 2019, 375, 48-53.	2.0	10
154	Synergistic combination of carbon-black and graphene for 3D printable stretchable conductors. Materials Technology, 2020, , 1-10.	1.5	10
155	Directional Exciton Migration in Benzoimidazole-Based Metal–Organic Frameworks. Journal of Physical Chemistry Letters, 2021, 12, 4917-4927.	2.1	10
156	<scp>Twoâ€Dimensional</scp> Cathode Materials for Aqueous Rechargeable <scp>Zincâ€ion</scp> Batteries ^{â€} . Chinese Journal of Chemistry, 2022, 40, 973-988.	2.6	10
157	Broadband white-light emission from a novel two-dimensional metal halide assembled by Pb–Cl hendecahedrons. Journal of Materials Chemistry C, 2022, 10, 9465-9470.	2.7	10
158	Ambipolar Charge Photogeneration and Transfer at GaAs/P3HT Heterointerfaces. Journal of Physical Chemistry Letters, 2014, 5, 1144-1150.	2.1	9
159	Enhancement of Room-Temperature Photoluminescence and Valley Polarization of Monolayer and Bilayer WS ₂ via Chiral Plasmonic Coupling. ACS Applied Materials & Interfaces, 2021, 13, 35097-35104.	4.0	9
160	Scalable Submicron Channel Fabrication by Suspended Nanofiber Lithography for Shortâ€Channel Fieldâ€Effect Transistors. Advanced Functional Materials, 2022, 32, 2109254.	7.8	9
161	Unique Reversible Crystal-to-Crystal Phase Transition—Structural and Functional Properties of Fused Ladder Thienoarenes. Chemistry of Materials, 2017, 29, 7686-7696.	3.2	8
162	Visualization of Charge Carrier Trapping in Silicon at the Atomic Surface Level Using Four-Dimensional Electron Imaging. Journal of Physical Chemistry Letters, 2019, 10, 1960-1966.	2.1	8

#	Article	IF	CITATIONS
163	Gentle Materials Need Gentle Fabrication: Encapsulation of Perovskites by Gas-Phase Alumina Deposition. Journal of Physical Chemistry Letters, 2021, 12, 2348-2357.	2.1	8
164	Multiple coupling in plasmonic metal/dielectric hollow nanocavity arrays for highly sensitive detection. Nanoscale, 2015, 7, 13495-13502.	2.8	7
165	Intriguing Ultrafast Charge Carrier Dynamics in Two-Dimensional Ruddlesden–Popper Hybrid Perovskites. Journal of Physical Chemistry C, 2021, 125, 9630-9637.	1.5	7
166	Elastomeric Nanodielectrics for Soft and Hysteresisâ€Free Electronics. Advanced Materials, 2021, 33, e2104761.	11.1	7
167	Modulation of singlet and triplet excited states through $\ddot{I}f$ spacers in ternary 1,3,5-triazines. RSC Advances, 2013, 3, 13782.	1.7	6
168	High-Responsivity Photodetector Based on a Suspended Monolayer Graphene/RbAg ₄ I ₅ Composite Nanostructure. ACS Applied Materials & Interfaces, 2020, 12, 50763-50771.	4.0	6
169	Single-Particle Spectroscopy as a Versatile Tool to Explore Lower-Dimensional Structures of Inorganic Perovskites. ACS Energy Letters, 2021, 6, 3695-3708.	8.8	6
170	A fused thieno[3,2-b]thiophene-dithiophene based donor molecule for organic photovoltaics: a structural comparative study with indacenodithiophene. Journal of Materials Chemistry C, 2016, 4, 9656-9663.	2.7	5
171	Dual-Mode Plasmonic Coupling-Enhanced Color Conversion of Inorganic CsPbBr ₃ Perovskite Quantum Dot Films. ACS Applied Materials & Interfaces, 2021, 13, 32856-32864.	4.0	5
172	Interface Engineering of Biâ€Fluorescence Molecules for Highâ€Performance Data Encryption and Ultralow UVâ€Light Detection. Advanced Optical Materials, 2022, 10, .	3.6	5
173	Imaging the Reduction of Electron Trap States in Shelled Copper Indium Gallium Selenide Nanocrystals Using Ultrafast Electron Microscopy. Journal of Physical Chemistry C, 2018, 122, 15010-15016.	1.5	4
174	Photophysical properties of chirality: Experimental and theoretical studies of (R)- and (S)-binaphthol derivatives as a prototype case. Chemical Physics, 2013, 412, 34-40.	0.9	3
175	Oxidized eutectic gallium–indium (EGaIn) nanoparticles for broadband light response in a graphene-based photodetector. Materials Advances, 2021, 2, 4414-4422.	2.6	3
176	Light-Trapping Engineering for the Enhancements of Broadband and Spectra-Selective Photodetection by Self-Assembled Dielectric Microcavity Arrays. Nanoscale Research Letters, 2019, 14, 187.	3.1	2
177	Effect of Zincâ€Doping on the Reduction of the Hotâ€Carrier Cooling Rate in Halide Perovskites. Angewandte Chemie, 2021, 133, 11052-11058.	1.6	2
178	Linked Nickel Oxide/Perovskite Interface Passivation for Highâ€Performance Textured Monolithic Tandem Solar Cells (Adv. Energy Mater. 40/2021). Advanced Energy Materials, 2021, 11, 2170160.	10.2	2
179	Ultrafast charge carrier dynamics in organic (opto)electronic materials. , 2013, , 318-355.		1
180	Understanding liquefaction in halide perovskites upon methylamine gas exposure. RSC Advances, 2021, 11, 20423-20428.	1.7	1

#	Article	IF	CITATIONS
181	Visible Range Plasmons in Topological Insulators. , 2016, , .		1
182	Cylindrical Al Nano-Dimer Induced Polarization in Deep UV Region. Nanoscale Research Letters, 2022, 17, .	3.1	1
183	Femtosecond to nanosecond excited states dynamics of novel Corroles. , 2014, , .		0
184	Plasmonics of topological insulators at optical frequencies. , 2017, , .		0
185	Small polarons in 2D perovskites. , 2017, , .		0
186	Plasmonic Properties and Photoinduced Reflectance of Topological Insulator. , 2014, , .		0
187	PHOTOINDUCED CHARGE TRANSFER DYNAMICS AT HYBRID GAAS/P3HT INTERFACES. , 2014, , .		0
188	Perovskite Metamaterials. , 2016, , .		0
189	Ballistic Carrier Diffusion on Semiconductor Surfaces Uncovered by 4D Electron Microscopy. , 0, , .		0
190	Halogen migration and surface degradation in hybrid perovskites (Conference Presentation). , 2018, , .		0
191	Topological Insulator Chalcogenides for Infrared Dielectric Metamaterials. , 2020, , .		Ο